Density Functional Theory Study of the Interaction of Cu, Ag, and Au Atoms with the Regular CeO_2 (111) Surface

María Marta Branda,[†,‡] Norge C. Hernández,[§] Javier Fdez. Sanz,[||] and Francesc Illas*[,†]

Departament de Química Física and Institut de Química Teòrica i Computacional (IQTCUB), Universitat de Barcelona, C/ Martí i Franquès 1, 08028 Barcelona, Spain, Departamento de Física, Universidad Nacional del Sur, 8000 Bahía Blanca, Argentina and Consejo Nacional de Investigaciones Científicas y Tecnológicas, Argentina, Departamento de Física Aplicada I, Escuela Universitaria Politécnica, Universidad de Sevilla, E- 41011 Sevilla, Spain, and Departamento de Química Física, Facultad de Química, Universidad de Sevilla, E-41012 Sevilla, Spain

Received: November 12, 2009; Revised Manuscript Received: December 21, 2009

The interaction of Cu, Ag, and Au atoms with the regular terrace sites of the CeO_2(111) surface has been investigated within the LDA+U and GGA+U density functional theory approaches using different U values and periodic slab surface models. For the interaction of Cu and Ag with this surface the different methods consistently predict the same qualitative description of stable active sites, the same order of stability and the oxidized character of adsorbed Cu and Ag. For the case of Au the description is more method dependent due to the nearly degeneracy between the solutions between cationic and neutral Au, in agreement with a recent study. The present results are indicative of the strength and limitations of the present density functional theory approaches.

1. Introduction

Cerium oxides, either CeO_2 or nonstoichiometric CeO_{2-x} particles, hereafter referred to generically as ceria, are important components of catalysts used in several chemical reactions. They are widely used as promoters in the so-called "three-way catalysts" for the elimination of toxic exhaust gases in automobiles.[1] Initially, the promoting effect of ceria was attributed to the enhancement of the metal dispersion and the stabilization of the support toward thermal sintering.[2,3] However, subsequent work has shown that ceria can act as a chemically active component as well, working as an oxygen reservoir able to release it in the presence of reductive gases and to supply it upon interaction with oxidizing gases.[4−6] The broad use of ceria in oxidation reactions is due to its facile $Ce^{3+}-Ce^{4+}$ redox process.[7]

Ceria itself is not selective, but its properties can be tuned by doping or acting as support of various metals such as Cu, Ag, or Au although the activity and selectivity of the doped ceria lattice depend strongly on the dopant type and concentration.[8−11] Recently it has been shown that ceria plays a key role in the water−gas shift reaction,[12] while its activity in the decomposition of nitrogen oxides has been known since the work of Martinez-Arias et al. back in 1995.[13] That ceria is not a mere spectator is clear from experiments carried on Rh/CeO_2 and on pure CeO_2 revealing striking differences.[14,15] The very recent work of Park et al.[16] and of Rodriguez et al.[17] illustrates the importance of stabilizing Ce^{3+} centers[12] and the role of the ceria nanoparticles. In part, the better catalytic activity of metal/oxide systems has been attributed to the role of subsurface oxygen which can strongly facilitate the catalytic reactions.[18−21]

In the case of Cu/CeO_2 systems, the formation of intimate contacts between both components is thought to be of fundamental importance in explaining the remarkably high activities exhibited by these catalysts for ethanol synthesis[22] or for carbon monoxide oxidation[23−25] where small amounts of Cu promote CeO_2 catalytic activity by several orders of magnitude.[26−32] Cu/ceria has also been identified as one of the promising candidates for cost-effective WGS catalyst and showed a good performance in the WGS reaction at both low-[33−37] and high-temperature regimes[38] and reported to be highly active in preferential CO oxidation for CO cleanup.[39−43] Finally, it is worth pointing out that Cu/CeO_2 is effective for the removal or destruction of SO_2 evidencing that the chemistry of SO_2 on the Cu-promoted CeO_2 was much richer than on pure CeO_2.[44]

The exciting result that gold nanoparticles exhibit unusual catalytic properties in various reactions[45−48] has also triggered substantial interest in the Au/ceria system which indeed displays outstanding catalytic properties.[49,50] Several studies on model systems have given fundamental knowledge on relationships between the atomic structure and the chemical properties of supported gold clusters.[51−56] In particular, scanning tunneling microscopy (STM) studies[57,58] suggest that gold interacts strongly with defects on terraces typically associated with oxygen vacancies. In a similar way, Weststrate et al.[59] have studied the electronic structure of Au particles on CeO_2(111) films and CO adsorption thereon using X-ray photoelectron spectroscopy (XPS) with synchrotron light. The results are consistent with previous observations that CO adsorbs primarily on low-coordinated sites on gold particles.[48,60] Morphology, electronic structure, and CO adsorption of gold supported on well-ordered CeO_2(111) thin films and CeO_x nanoparticles were studied by STM, XPS, and infrared reflection absorption spectroscopy (IRAS).[61] These experiments also found that upon deposition on CeO_2(111) films, most of the Au particles are

* To whom correspondence should be addressed. E-mail: francesc.illas@ub.edu.
† Universitat de Barcelona.
‡ Universidad Nacional del Sur.
§ Departamento de Física Aplicada I, Universidad de Sevilla.
|| Departamento de Química Física, Facultad de Química, Universidad de Sevilla.

10.1021/jp910782r
Published on Web 01/11/2010

formed at the step edges which is also in nice agreement with the theoretical predictions of Castellani et al.[62] The experimental results of Baron et al.[61] strongly suggest that the oxidation state of Au atoms adsorbed on perfect CeO_2(111) single crystal surfaces is essentially zero and that low coordinated Ce atoms are required to produce the redox reaction where Ce^{4+} is reduced to Ce^{3+} whereas Au^0 is oxidized to Au^{1+}. We close this description of the main results concerning the catalytic systems involving coinage metals and ceria by mentioning that, contrarily to the case of Cu and Au, the information regarding Ag/ceria is less abundant and related mainly to its use as catalysis for methane oxidation.[63−65]

The considerable interest in the Cu/ceria and Au/ceria systems briefly outlined above has also triggered a substantial research from the theoretical point of view. However, this has proven to be more complicated than could be anticipated from the experience on similar metal−oxide systems.[66,67] In fact, standard density functional calculations fail to properly describe the localized character of 4f electrons in reduced ceria whereas more elaborated methods such as the LDA+U or GGA+U approaches and hybrid functionals solve this problem resulting in a proper description.[68−71] However, recent theoretical studies on the interaction of Au atoms with the regular CeO_2(111) surface have generated a considerable controversy regarding the oxidations state of adsorbed Au.[62,72,73] A recent systematic periodic density functional theory (DFT) study comparing carefully the effect of various choices in the construction of the surface model and on the particular choice of the density functional approach has revealed the intricate relationship between the choice of the exchange correlation potential and the surface model setup.[74] For Au on CeO_2(111) at top oxygen sites, LDA+U, GGA+U, and hybrid density functional methods are capable to find solutions with either neutral and oxidized gold. However, the character of the ground state strongly depends on the exchange-correlation potential used. Consequently, the qualitative picture depends on the method used thus casting reasonable doubts on theoretical results obtained without enough careful control of the many possible and not always obvious choices. In any case, the energy difference between the calculated solutions corresponding to neutral and cationic Au adsorbed at the regular CeO_2(111) surface appears to be fairly small strongly suggesting the presence of a statistical distribution of the two species, at the most stable adsorption site, as a function of temperature.

The dependence of the description of the interaction of Au with CeO_2(111) with the density functional method and with the choice of the materials model is rather disturbing since it seems to indicate that present theoretical methods are not at the level of accuracy necessary to describe these systems. In order to investigate whether the case of Au is the rule or instead the exception we have undertaken a systematic study of adsorption of Cu and Ag on the perfect CeO_2(111) surface. We will present compelling evidence that Au is a particular case and that, within reasonable choices, present methods lead to the same qualitative picture for the rest of coinage metal atoms.

2. Computational Details

Periodic DFT based spin polarized calculations have been carried out to study the interaction between coinage atoms (Cu, Ag, and Au) with the perfect CeO_2(111) surface. The calculations have been carried out with the Vienna ab initio simulation package (VASP).[75−77] This code solves the Kohn−Sham equations for the valence electron density within a plane wave basis set and makes use of the projector augmented wave (PAW) method to describe the interaction between the valence electrons and the atomic cores.[78,79] The PAW method can be considered as an all electron frozen core approach which considers the exact shape of the valence wave functions instead of pseudowave functions. The valence electron density is defined by the twelve ($5s^25p^6$, $6s^25d^14f^1$) electrons of each Ce atom, the six ($2s^2$, $2p^4$) electrons of each O atom, and the eleven ($4s^13d^{10}$, $5s^14d^{10}$, $6s^15d^{10}$) electrons of Cu, Ag, and Au. The plane-wave expansion includes all plane waves with kinetic energy smaller than a cutoff value chosen as 415 eV, which ensures adequate convergence with respect to the basis set.

The LDA+U or GGA+U approaches[80−82] were chosen to account for exchange and correlation. The LDA (local density approximation) and GGA (generalized gradient approximation) part of these functionals are those of Vosko et al.[83] (VWN) and Perdew−Wang (PW91),[84,85] respectively. In the LDA+U (and GGA+U) method part of the self-interaction energy is corrected by explicit inclusion of a Hubbard like U_{eff} term (hereafter referred to simply as U) for the 4f electrons penalizing double occupancy of this atomic level. In the present work, the formalism due to Dudarev et al.[86] has been chosen, which makes use of a single U_{eff} parameter. The choice of this type of method is supported by previous studies on ceria systems that have shown a very good agreement with available results for bulk ceria.[68−70] Numerical integration in the reciprocal space was carried out using a of 4 × 4 × 1 Monkhorst-Pack special k-points grid.[87] A Methfessel-Paxton smearing width $\sigma = 0.2$ eV was applied to help to converge the electronic density although all total energies here reported correspond to $\sigma \rightarrow 0$ eV.[88]

To take advantage of the experience gained in the systematic study of Au on CeO_2(111)[74] geometry optimization has been performed within the LDA+U with $U = 5$ eV scheme because it provides a lattice parameter which is close to experiment whereas energies, magnetic moments and Bader charges[89] were calculated at the GGA+U level with $U = 3$ eV. We will refer to these results as (L5)L5//G3 to indicate that lattice parameter and geometry optimization are carried out at the LDA+U ($U = 5$ eV) level whereas the energy and electronic properties arise from single point calculations at the GGA+U ($U = 3$ eV) level. This choice allows one to properly describe localization in bulk Ce_2O_3[68] as well as in ceria nanoparticles containing both Ce^{3+} and Ce^{4+} atoms.[90−93] Note that this procedure is different from the standard approach consisting in using GGA+U to obtain the lattice parameter used to construct the slab model, to carry the geometry optimization, and to compute energies and properties. Most often the GGA+U calculations encountered in the literature are carried out using a value of $U = 5$ eV as suggested initially by Nolan et al.[94] to obtain localized solutions arguing that smaller values could not be able to produce a localized solution. To investigate the effect of this choice of the final picture of adsorbed Cu and Ag on CeO_2(111), GGA+U calculations with $U = 5$ eV have also been carried out for both geometry optimization and energy evaluation. We will denote this set of calculations as (G5)G5//G5. However, one must recall that the latter approach is known to predict a lattice parameter for bulk CeO_2 1.3% larger than the experiment. Although this difference might appear negligible it has been shown to have a neat effect on the predicted oxidation state of adsorbed Au.[74] Therefore, we have decided to include results from a set of (L5)L5//L5 calculations, which, on the one hand, uses a lattice parameter consistent with the method used to compute the energy and the electronic properties (as in the (G5)G5//G5 approach) and, on the other hand, a value of U that is enough to lead to localized solutions for the 4f electrons, at least on

Ce_2O_3.[68] Clearly, the (L5)L5//L5 will lead to too large values of the adsorption energy but the combined use of the three approaches will allow us to reach definite conclusions about the adsorption of Cu, Ag and Au on the active sites of the regular $CeO_2(111)$ surface.

To model the O-terminated $CeO_2(111)$ surface slab models with different thickness have been employed. Previous tests on isolated surfaces have shown that in models containing up to 15 atomic layers only the 3 uppermost layers featured significant relaxation.[74] In the present work we have also tested the effect of an adatom (Cu) on 6 and 9 atomic layers allowing the relaxation of 3 and 6 layers, respectively, and found that the adsorption energy is converged to ~5%. Therefore, a Ce_8O_{16} 2 × 2 supercell with 6 layers has been used keeping the three bottom layers fixed and relaxing the uppermost ones. With this model, the resulting coverage of the adsorbed metal atom was $\theta = 0.25$. Here it is important to stress that the slab model was cut from the bulk cubic (*Fm3m*) CaF_2 structure using the optimized lattice parameter values a_0 of 5.40 and 5.49 Å as obtained from (L5)L5 and (G5)G5. Note that the former value for a_0 is in excellent agreement with the results predicted from hybrid DFT calculations,[70,71] which in turn coincides with experimental available results of $a_0 \approx 5.41$ Å (5.406(1) Å[95] or 5.411(1) Å[96]). The supercell includes a vacuum of 12 Å which is large enough to avoid interaction between the slabs obtained after replication in the three space dimensions.

To locate the most stable adsorption site, calculations were carried out starting from all high symmetry adsorption sites. The metal atom was placed above one side of the slab only and its geometry was completely relaxed without symmetry restrictions. The adsorption energy (E_{ads}) was calculated as usual as the difference between the energy of the adsorbed metal atom on the surface ($E_{adsorbate-surface}$) and the sum of the free surface slab ($E_{surface}$) and the isolated metal atom ($E_{isolated\ atom}$) energies. A negative value indicates an exothermic adsorption process.

3. Results and Discussion

From the several initial starting geometries five energetically stable sites were investigated and located by means of the (L5)L5//G3 and (G5)G5//G5 approaches for the adsorption of Cu atoms on the $CeO_2(111)$ perfect surface, as discussed in detail below. The geometries thus found were further characterized as minima in the potential energy surface by pertinent vibrational analysis. For Cu and Ag, the three approaches—(L5)L5//G3, (G5)G5//G5, and (L5)L5//L5—lead to the same order of stability for the different sites, and all of them also agree with the prediction that the adsorbed metal atom will become oxidized with a concomitant reduction of the ceria surface. However, the picture of the electronic structure is slightly dependent on the method in the sense that both (L5)L5//L5 and (G5)G5//G5 indicate a clear reduction of just one Ce^{4+} cation to Ce^{3+}, whereas in the case of (L5)L5//G3 the spin density is more delocalized indicating that while GGA+*U* with $U = 5$ eV correctly leads to localized solution for Ce^{3+}, although it has been claimed that this *U* value may be too large to provide a balanced description.[68] On the other hand, the $U = 3$ eV value suggested to provide a balanced description of CeO_2 and Ce_2O_3 seems to be perhaps too small to find sufficiently localized solutions. In the case of Au the trends are not so clear as we will show in detail below.

In the case of Cu, five stable configurations have been found with the Cu atom having 1-fold (O_u and O_u-O_d), 2-fold (O_u-O_u), and 3-fold coordination (O_d and Ce), which are schematically shown in parts a−e of Figure 1, respectively. In the most stable O_d site, Cu is located directly above an oxygen atom of the third atomic layer and coordinated to three O atoms of the first atomic layer (Figure 1d). The next most stable site is O_u-O_u where Cu sits above an oxygen atom of the third atomic layer but almost placed at bridge between two oxygen atoms of the first layer (Figure 1c). This is followed by the O_u site with Cu directly on top of an oxygen atom of the first atomic layer (Figure 1a), theO_u-O_d (Figure 1b) with Cu bridging two Ce atoms of the second layer or between an oxygen of the first layer and an oxygen of the third layer and the Ce site (Figure 1e) with Cu above a Ce atom of the second atomic layer. The adsorption energy at these sites varies considerably from site to site, and it is physically meaningful to focus on the most stable ones only. Nevertheless, the complete set of results in Table 1 allows one to investigate the effect of the density functional method used. Since the main differences appear not only in the adsorption energy but also in the degree of charge transfer from the metal to the surface, we also report net charges for Cu obtained after a Bader analysis of the (L5)L5//G3 and (G5)G5//G5 electron densities. The (L5)L5//L5 values only show a more marked tendency to predict oxidation of Cu upon adsorption and a stronger localization of the transferred electron into one Ce atom only. In Table 1 the magnetic moments on Cu and Ce atoms (μ_{Cu} and μ_{Ce}) obtained from the (L5)L5//G3 calculations and the distances between Cu and the nearest surface O atoms (d_{Cu-O}) and between Cu and the nearest surface Ce atoms (d_{Cu-Ce}), respectively are also reported.

All methods used in this work predict that the most stable site for Cu adsorption is O_d involving a 3-fold coordination, with an adsorption energy of −1.86, −2.79, and −3.47 eV, for the (L5)L5//G3, (G5)G5//G5, and (L5)L5//L5 methods, respectively. The next site, in order of stability, is the 2-fold O_u-O_u with a calculated value of the adsorption energy 0.25−0.92 eV smaller, also depending on the functional. Although 0.25 eV is a difference small enough to indicate that it may become occupied at a sufficiently large Cu coverage, one must also realize that at these conditions it is likely that Cu clusters start to grow and that the sites with smaller values of the adsorption energy will not be occupied. Therefore, the rest of adsorption sites investigated all have considerably smaller values of the adsorption energy and will not be discussed further. It is important to point out again that in spite of the rather large differences in the adsorption energies predicted by the three series of calculations the trends concerning the order of stability are the same, and this is also the case for the final oxidation state of the adsorbed Cu atom. In fact, all calculations consistently predict that the Cu atom always oxidizes to Cu^+ when adsorbed on the perfect $CeO_2(111)$ except for the least stable Ce site. This is clear from the respective values of Bader charges and magnetic moments; Q_{Cu} varies from ~ +0.3 to ~ +0.7, and μ_{Cu} are equal or very close to 0.0. The larger adsorption energy for the O_d site is consistent with an electrostatic interaction between Cu^+ and the negatively charged O surface anions; this is maximized at the 3-fold site as previously found for Cu on TiO_2 and Al_2O_3.[97−100] Note that at this site the metal lost electron is partially delocalized on three Ce neighbors indicating that the U_{eff} value of 3 eV is perhaps a bit too small (Table 1). In fact, both (L5)L5//L5 and (G5)G5//G5 calculations predict that Cu adsorbs as Cu^+ and the transferred charge is more localized. Here, it is worth pointing out that various solutions with the electron transferred to the ceria surface are found in the (G5)G5//G5 series of calculations differing in the Ce atom where the electron localizes. Table 1 reports the most stable one for each case where reduction

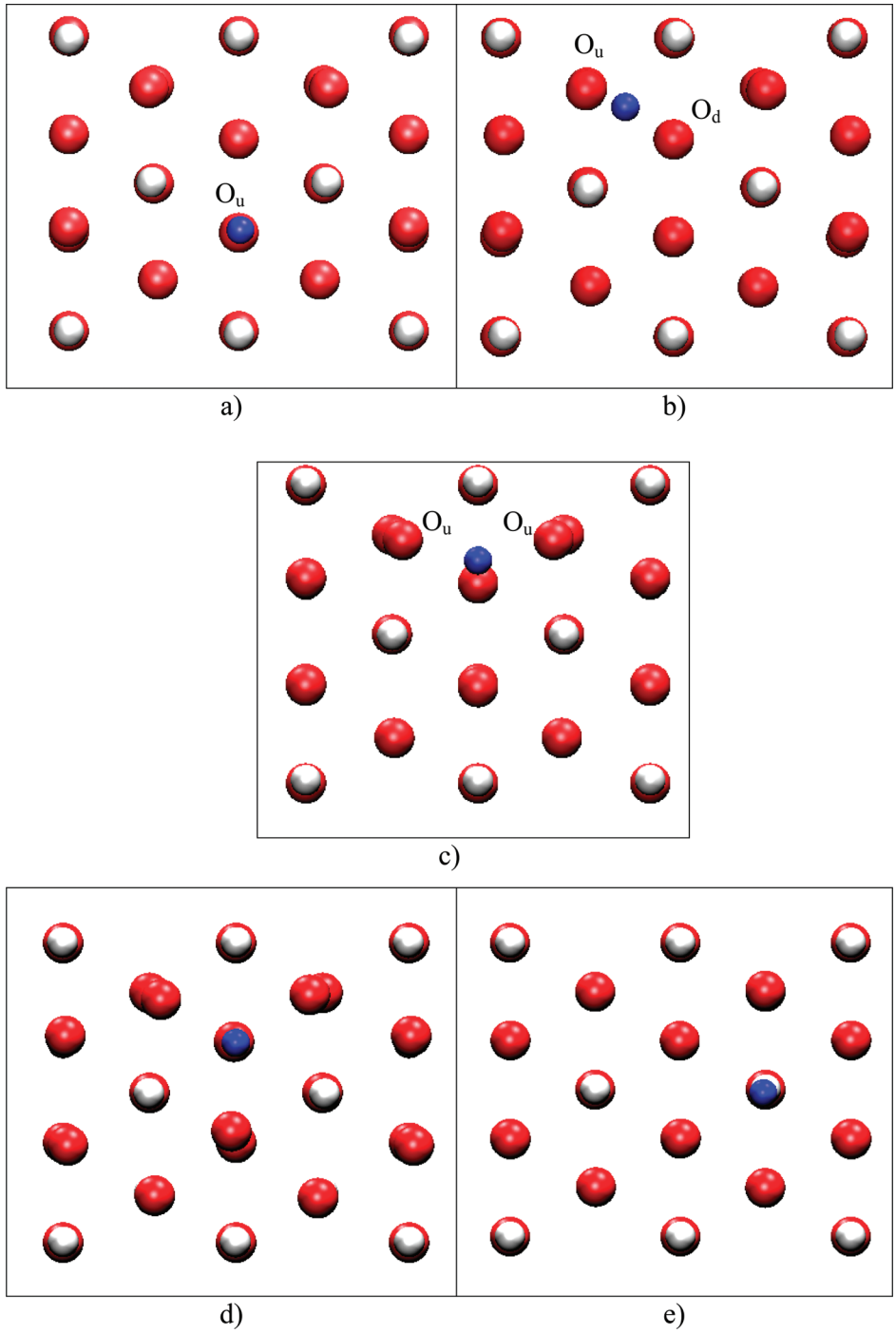

Figure 1. Possible adsorption sites for Cu, Ag, and Au (blue sphere) on the relaxed 2 × 2 CeO_2 unit cell model representing the perfect CeO_2(111) surface. O and Ce atoms are red and white spheres, respectively. According to the figure, the metals were deposited on: (a) O_u (1-fold), (b) O_u−O_d (1-fold), (c) O_u−O_u (2-fold), (d) O_d (3-fold), and (e) Ce (3-fold).

involves a surface Ce atom which coincides with one of those closest to the Cu adatom, as expected from electrostatic arguments. This can be deduced by comparison to previous work for CeO_2 and Ce_2O_3 where the topological features of the electron localization function[101] (ELF) basins for Ce^{4+} and Ce^{3+} are clearly different and easy to recognize.[68] This comparison allows one to interpret the ELF map in Figure 2 corresponding to the adsorption of Cu above the O_d site. This map shows two types of Ce atoms, for instance, the two equivalent Ce atoms near to Cu which are identified as Ce^{4+} and one atom with a deformed ELF contour which is reminiscent of Ce^{3+}.[90] Note, that due to periodic symmetry the Ce^{3+} ion in Figure 2 is not one of the three closer cerium atoms to the Cu atom if the unit cell is replicated which is in full agreement with the results reported by Ganduglia-Pirovano et al. for oxygen vacancies in ceria.[102]

We can now compare the Cu/CeO_2(111) interacion energies with those estimated for TiO_2(110) and α-Al_2O_3(0001), also from periodic wave-plane DFT calculations. For alumina, the adsorption energy is computed to be 1.09 eV, with Cu^+ ion 3-fold bound to surface oxygen atoms.[100] In the case of the TiO_2(110) surface a three-layer slab (each layer consisting of three atomic planes) gives an adsorption energy of 2.39 eV, while our best estimate, using a 4 × 2 cell six-layer thick (actually 18 atomic planes), is 1.76 eV.[103] Disregarding the differences arising from the slab model used, it clearly appears

TABLE 1: Main Electronic Properties Corresponding to the Interaction of Cu on CeO_2(111) as Predicted from (L5)L5//G3 Calculations[a]

	O_d (3-fold)	O_u−O_u (2-fold)	O_u (1-fold)	O_u−O_d (1-fold)	Ce (3-fold)
E_{ads} (eV)	**−1.86**	−1.61	−1.50	−1.25	−0.42
	(−2.79)	(−2.15)	(−1.74)	(−0.71)	(−0.32)
	[**−3.47**]	[−2.55]	[−2.03]	[1.94]	[−0.75]
Q_{Cu}	+0.70	+0.58	+0.29	+0.40	+0.20
	(+0.71)	(+0.64)	(+0.32)	(+0.25)	(+0.13)
μ_{Cu} (μ_B)	0.00	0.00	0.08	0.06	0.28
μ_{Ce} (μ_B)	0.16	0.28	0.18	0.74	0.14
	0.19	0.30	0.16		
	0.34	0.45	0.22		
d(Cu−O) (Å)	2.01	1.89 × 2	1.73	1.75	2.77
	2.04 × 2	2.99		3.58	2.90
					2.97
d(Cu−Ce) (Å)	2.78 × 2	2.61	3.57	3.19	2.69
	2.79	3.13 × 2	3.61	3.26	
			3.65		

[a] E_{ads} stands for the adsorption energy with respect to the isolated Cu and the bare slab model, Q_{Cu} is the Bader net charge on adsorbed Cu, μ_{Cu} and μ_{Ce} are the corresponding magnetic moments, and d_{Cu-O} and d_{Cu-Ce} correspond to the distances between Cu and the nearest surface O atoms and Cu and the nearest surface Ce atoms, respectively. Adsorption energies between parentheses and brackets correspond to the results predicted by (G5)G5//G5 and (L5)L5//L5, respectively. Numbers in bold denote the most stable site. Note that for isolated Cu one has $\mu_{isol\_Cu} = 0.31\ \mu_B$.

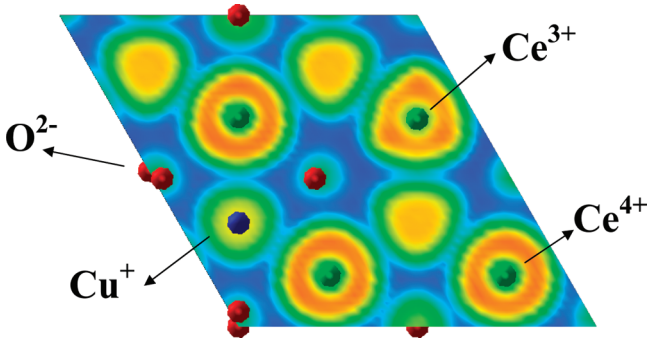

Figure 2. Electron localization function contour map for Cu adsorbed on the O_d site of the CeO_2(111) surface. The contour is plotted for the (111) plane containing the first-layer Ce atoms.

that the more reducible titania surface leads to stronger interactions, as for Cu to be oxidized the surface needs to accommodate the extra electron. As far as ceria is considered, given its higher reducible nature, one would expect to have even larger values for the interaction energy. In this sense, the value of −1.86 eV appears to be somewhat low, while the −2.79 eV might appear overestimated. The value of −3.47 eV (L5)L5//(L5) should not be used in this comparison because the adsorption energies for Cu on TiO_2 above-mentioned were obtained with the GGA exchange-correlation potential, and it is well-known that LDA has a marked tendency to overestimate bonding energies in general and adsorption energies in particular. That the adsorption energy is tightly related to the charge transfer from Cu to the surface is neatly substantiated by the nice correlation observed between the adsorption energy and the Cu Bader charges. For instance, taking the (G5)G5//(G5) series (values between parentheses in Table 1), one can see that the Cu charge Q_{Cu} smoothly drops as the adsorption energy decreases.

In the case of Ag adsorption on CeO_2(111), all possible sites have been considered as in the case of Cu. However, in this

TABLE 2: Main Electronic Properties Corresponding to the Interaction of Ag on CeO_2(111) as Predicted from (L5)L5//G3 Calculations[a]

	O_d (3-fold)	O_u (1-fold)
E_{ads} (eV)	**−1.00**	−0.56
	(**−1.55**)	(−0.87)
	[**−2.20**]	[−1.08]
Q_{Ag}	+0.56	+0.34
	(+0.74)	(+0.51)
μ_{Ag} (μ_B)	0.00	0.07
μ_{Ce} (μ_B)	0.89	0.64
d_{Ag-O} (Å)	2.28 × 3	2.01
d_{Ag-Ce} (Å)	3.07 × 3	3.65
		3.75
		3.81

[a] E_{ads} stands for the adsorption energy with respect to the isolated Ag and the bare slab model, Q_{Ag} is the Bader net charge on adsorbed Ag, μ_{Ag} and μ_{Ce} are the corresponding magnetic moments, and d_{Ag-O} and d_{Ag-Ce} correspond to the distances between Ag and the nearest surface O atoms and Ag and the nearest surface Ce atoms, respectively. Adsorption energies between parentheses and brackets correspond to the results predicted by (G5)G5//G5 and (L5)L5//L5, respectively. Numbers in bold denote the most stable site. Note that for isolated Cu one has $\mu_{isol\_Ag} = 0.27\ \mu_B$.

case geometry optimization starting from the different possible sites discussed in the previous section (see also Figure 1) converge to two different sites only. It is important to remark that this behavior is found for the three different approaches considered in the present work and that all attempts to locate other stable positions for Ag adsorbed on CeO_2(111) failed. The two stable sites found for adsorbed Ag are the O_d and O_u sites clearly shown in Figure 1. Moreover, the predicted order of stability is the $O_d > O_u$, and this is equally predicted by the three methods. It is also worth to point out that for both sites, the three types of calculations predict that there is always some charge transfer from Ag to the surface with a concomitant reduction of one Ce surface atom. This is clear from the analysis of the Bader charges and is consistent with the calculated magnetic moments reported in Table 2. This explains that the most favorable adsorption site involves the interaction with three surface O atoms. This result is not surprising at all; it maximizes the electrostatic attractive interaction between the adatom and the surface. Again, the more localized solutions are found with the (L5)L5//L5 and (G5)G5//G5 approaches. Note also that for Ag on CeO_2(111), the adsorption energies found for the most stable site using the GGA functional are −1.00 and −1.55 eV, which are significantly lower than those of Cu discussed in the previous paragraphs. This lowering of the interaction energy agrees with that estimated also using a GGA functional in the Ag/α-Al_2O_3 and Ag/TiO_2 systems (−0.61 and −1.25 eV, respectively).[99] Notice again as the larger reducibility of ceria makes the metal surface-interaction to increase.

We finish the discussion by briefly describing the main conclusions of a previous systematic study for Au on CeO_2(111)[74] together to the main findings of earlier or almost simultaneous work.[73,104] Castellani et al.[62] recently predicted three stable sites for gold adsorption and suggested that, upon adsorption on the regular CeO_2(111) surface, Au remains neutral. Subsequent work reported results showing a new site at bridge between two O atoms of the surface and predicted Au oxidation upon interaction with the surface.[73,104] In the present work we have carried out an additional detailed exploration using the three methodologies with several starting positions for the Au atoms and allowing geometry relaxation without symmetry

TABLE 3: Main Electronic Properties Corresponding to the Interaction of Au on CeO_2(111) as Predicted from (L5)L5//G3 Calculations[a]

	O_u−Ce (1-fold)	O_u (1-fold)	O_d (3-fold)	O_u−O_u (2-fold)	Ce (3-fold)
E_{ads} (eV)	**−0.71**	−0.66	−0.51	−0.43	−0.35
	(−0.75)	(−0.96)	(−0.61)	(**−1.15**)	(−0.38)
	[−1.36]	[−1.26]	[−1.43]	[**−1.47**]	[−0.88]
Q_{Au}	−0.03	−0.04	0.00	+0.33	−0.04
	(−0.06)	(+0.33)	(−0.08)	(+0.34)	(−0.07)
μ_{Au} (μ_B)	0.33	0.31	0.25	0.00	0.37
μ_{Ce} (μ_B)	0.12	<0.1	0.14	0.47 × 2	<0.1
d(Au−O) (Å)	2.11	2.07	2.56	2.15 × 2	2.34 × 3
			2.58		
			2.63		
d(Au−Ce) (Å)	3.00	3.62 × 2	3.05	2.76	2.80
		3.63	3.08	3.25 × 2	
			3.10		

[a] Geometrical data were taken from (L5)L5//L5 ones. E_{ads} stands for the adsorption energy with respect to the isolated Au and the bare slab model, Q_{Au} is the Bader net charge on adsorbed Au, μ_{Au} and μ_{Ce} are the corresponding magnetic moments, and d_{Au-O} and d_{Au-Ce} correspond to the distances between Au and the nearest surface O atoms and Au and the nearest surface Ce atoms, respectively. Adsorption energies between parentheses and brackets correspond to the results predicted by (G5)G5//G5 and (L5)L5//L5, respectively. Numbers in bold denote the most stable site. Note that for isolated Cu one has $\mu_{isol\_Au} = 0.44\ \mu_B$.

restrictions. In this way five energetically stable sites were found for the adsorption of Au atoms on the CeO_2(111) perfect surface, namely, O_u, O_d, Ce, and O_u-O_u (Figure 1 and Table 3), which are almost the same as those found for Cu and a fifth site named O_u-Ce where the Au atom sits above the bridge site between Ce and O_u. These results agree well with those reported by Zhang et al.[72] and Hernandez et al.,[73] but in contrast to the cases of Cu and Ag described above, here there is a discrepancy in the order of the energetic stabilities. In fact, the (L5)L5//G3 calculations predict that Au prefer to adsorb on the O_u−Ce and O_u 1-fold sites with close value of the adsorption energy. However, while the (L5)L5//G3—and also the (L5)L5//L5 and (G5)G5//G5—calculations for Cu and Ag on CeO_2(111) clearly predict that these atoms adsorb as Cu^+ and Ag^+, respectively, the same level of calculation clearly predicts that adsorbed Au remains neutral. In addition, this is in contrast to what is predicted by the G5(G5)//G5 calculations where adsorption is preferred at the O_u−O_u and O_u, 2-fold and 1-fold sites, respectively, and Au is predicted to be partially oxidized. The reasons behind this different description have been investigated in detail recently and been attributed mostly to the use of a somewhat expanded lattice (compared to experiment) in the (G5)G5//G5 calculations, to a lesser extent to the use of a larger U value which favors Au oxidation and also to the fact that the states with Au^0 and Au^+ are very close in energy.[74]

From the main trends equally predicted by the three computational approaches explored in the present work one can firmly establish that order on the adsorption energy follows the Cu > Ag > Au trend, that Cu and Ag are always oxidized, and that Au oxidation is less likely which is in agreement with the order of ionization potentials[105] and with recent experimental data.[61] This is also consistent with the trend corresponding to adsorption of these metal atoms on MgO(100),[106] TiO_2,[97] Al_2O_3,[107] and SiO_2.[108]

4. Conclusions

The interaction of Cu, Ag, and Au atoms with the regular terrace sites of the CeO_2(111) surface has been investigated by means of periodic density functional theory based calculations using three different types of computational strategies all including the Hubbard correction to the Ce(4f) levels, either LDA+U or GGA+U, differing essentially in the way the slab surface model is constructed and on the value of the effective U parameter. The difference in the surface model arises from the different prediction of the lattice parameter already found for the standard LDA and GGA levels, the former leading to a value closer to experiment, whereas the latter leads to a lattice constant 1.3% larger. The difference in the U value chosen may have implications on the relative energy difference between the two states where the adsorbed metal atom is positively charged or it remains neutral, especially in the case of Au. Also, when the adatom is positively charged, the U value affects the localization of the transferred electron on one o more Ce surface atoms.

For the interaction of Cu and Ag with this surface all methods—(L5)L5//G3, (G5)G5//G5, and (L5)L5//L5—lead to the same qualitative description of stable active sites, of the stability order of these sites, and of the oxidized character of adsorbed Cu and Ag although with rather different adsorption energy values, whereas in the case of Au the final description is more method dependent, in agreement with recent work. The fact that all methods consistently predict that interaction of Cu, Ag, and Au with CeO_2(111) will result in oxidized Cu^+ and Ag^+ surface species and a statistical distribution of neutral and charged Au is nevertheless indicative of the strength and limitations of the present density functional theory approaches. Further arguments either from more accurate calculations or from experiment are needed to clarify this issue.

To conclude, compared to the case of Au on CeO_2(111), the interaction of Cu and Ag atoms with the same surface is found to be much less sensitive to the details of the density functional method used and to the way the surface slab model is constructed indicating that the problems encountered in the study of the interaction of Au with this surface are the exception rather than the rule and arise from the proximity of the energy corresponding to the solutions for neutral and oxidized supported Au. For larger particles, even of Au, the effect of the charge is likely to be less important due to the screening effects induced by a large particle. This implies that the present density functional theory based approaches, either of the +U or hybrid type, are adequate to describe this type of systems. We feel this is an important conclusion for scientist aiming to model supported metal particles on ceria and their reactivity.

Acknowledgment. MMB thanks the Invited Professorship fellowship (Grant 2008PIV0025) program of the Generalitat de Catalunya for making her visit to Barcelona possible. This study has been supported by the CONICET-Argentina, Spanish Ministry of Science and Innovation (MICINN grants FIS2008-02238, MAT2008-04918), Generalitat de Catalunya (grants 2009SGR1041 and XRQTC), and by the COST-D41 action. Computational time on the MareNostrum supercomputer of the Barcelona Supercomputing Center/Centro Nacional de Supercomputación is gratefully acknowledged.

References and Notes

(1) Trovarelli, A. *Catal. Rev. Sci. Eng.* **1996**, *38*, 439.
(2) Dictor, R.; Roberts, S. *J. Phys. Chem.* **1989**, *93*, 5846.
(3) Su, E. C.; Rothschild, W. G. *J. Catal.* **1986**, *99*, 506.
(4) Yao, H. C.; Yu Yao, Y. F. *J. Catal.* **1984**, *86*, 254.
(5) Engler, B.; Koberstein, E.; Schubert, P. *Appl. Catal.* **1989**, *48*, 71.

(6) Miki, T.; Ogawa, T.; Haneda, M.; Kakuta, N.; Ueno, A.; Tateishi, S.; Matsuura, S.; Sato, M. *J. Phys. Chem.* **1990**, *94*, 6464.
(7) Trovarelli, A.; de Leitenburg, C.; Boaro, M.; Dolcetti, G. *Catal. Today* **1999**, *50*, 353.
(8) Blank, J. H.; Beckers, J.; Collignon, P. F.; Clerc, F.; Rothenberg, G. *Chem.−Eur. J.* **2007**, *13*, 5121.
(9) Blank, J. H.; Beckers, J.; Collignon, P. F.; Rothenberg, G. *ChemPhysChem* **2007**, *8*, 2490.
(10) Jobbagy, M.; Marino, F.; Schobrod, B.; Baronetti, G.; Laborde, M. *Chem. Mater.* **2006**, *18*, 1945.
(11) Bera, P.; Aruna, S. T.; Patil, K. C.; Hegde, M. S. *J. Catal.* **1999**, *186*, 36.
(12) Park, J. B.; Graciani, J.; Evans, J.; Stacchiola, D.; Ma, S. G.; Liu, P.; Nambu, A.; Sanz, J. F.; Hrbek, J.; Rodriguez, J. A. *Proc. Natl. Acad. Sci.* **2009**, *106*, 4975.
(13) Martínez-Arias, A.; Soria, J.; Conesa, J. C.; Seoane, X. L.; Arcoya, A.; Cataluña, R. *J. Chem. Soc. Faraday Trans.* **1995**, *91*, 1679.
(14) Shido, T.; Iwasawa, Y. *J. Catal.* **1992**, *136*, 493.
(15) Shido, T.; Iwasawa, Y. *J. Catal.* **1993**, *141*, 71.
(16) Rodriguez, J. A.; Graciani, J.; Evans, J.; Park, J. B.; Yang, F.; Stacchiola, D.; Senanayake, S. D.; Ma, S.; Perez, M.; Liu, P.; Sanz, J. F.; Hrbek, J. Angew. Chem. Intl. Ed., DOI: 10.1002/anie.200903918.
(17) Rodriguez, J. A.; Ma, S.; Liu, P.; Hrbek, J.; Evans, J.; Perez, M. *Science* **2007**, *318*, 1757.
(18) Li, W.-X.; Stampfl, C.; Scheffler, M. *Phys. Rev. B* **2003**, *67*, 45408.
(19) Xu, Y.; Greeley, J.; Mavrikakis, M. *J. Am. Chem. Soc.* **2005**, *127*, 12823.
(20) Guzman, J.; Carrettin, S.; Corma, A. *J. Am. Chem. Soc.* **2005**, *127*, 3286.
(21) Fu, Q.; Saltsburg, H.; Flytzani-Stephanopoulos, M. *Science* **2003**, *301*, 935.
(22) Shaw, E. A.; Rayment, T.; Walker, A. P.; Lambert, R. M. *Appl. Catal.* **1990**, *67*, 151.
(23) Liu, W.; Sarofim, A. F.; Flytzani-Stephanopoulos, M. *Chem. Eng. Sci.* **1995**, *49*, 4871.
(24) Liu, W.; Flytzani-Stephanopoulos, M. *J. Catal.* **1995**, *153*, 304.
(25) Martínez-Arias, A.; Soria, J.; Cataluña, R.; Conesa, J. C.; Cortés Corberán, V. *Stud. Surf. Sci. Catal.* **1998**, *116*, 591.
(26) Liu, W.; Flytzani-Stephanopoulos, M. *Chem. Eng. J. Biochem. Eng. J.* **1996**, *64*, 283.
(27) Skarman, B.; Grandjean, D.; Benfield, R. E.; Hinz, A.; Andersson, A.; Wallenberg, L. R. *J. Catal.* **2002**, *211*, 119.
(28) Avgouropoulos, G.; Ioannides, T.; Matralis, H. K.; Batista, J.; Hocevar, S. *Catal. Lett.* **2001**, *73*, 33.
(29) Hungría, A. B.; Iglesias-Juez, A.; Martínez-Arias, A.; Fernández-García, M.; Anderson, J. A.; Conesa, J. C.; Soria, J. J. *J. Catal.* **2002**, *206*, 281.
(30) Jung, C. R.; Han, J.; Nam, S. W.; Lim, T.-H.; Hong, S.-A.; Lee, H.-I. *Catal. Today* **2004**, *93*, 183.
(31) Bera, P.; Aruna, S. T.; Patil, K. C.; Hegde, M. S. *J. Catal.* **1999**, *186*, 36.
(32) Wen, B.; He, M. *Appl. Catal., B* **2002**, *37*, 75.
(33) Yahiro, H.; Murawaki, K.; Saiki, K.; Yamamoto, T.; Yamaura, H. *Catal. Today* **2007**, *126*, 436.
(34) Li, Y.; Fu, Q.; Flytzani-Stephanopoulos, M. *Appl. Catal. B* **2000**, *27*, 179.
(35) Quiney, A. S.; Schuurman, Y. *Chem. Eng. Sci.* **2007**, *62*, 5026.
(36) Zheng, X.; Wang, S.; Wang, S.; Zhang, S.; Huang, W.; Wu, S. *Catal. Commun.* **2004**, *5*, 729.
(37) Tabakova, T.; Idakiev, V.; Papavasiliou, J.; Avgouropoulos, G.; Ioannides, T. *Catal. Commun.* **2007**, *8*, 101.
(38) Qi, X.; Flytzani-Stephanopoulos, M. *Ind. Eng. Chem. Res.* **2004**, *43*, 3055.
(39) Avgouropoulos, G.; Ioannides, T. *Appl. Catal. B* **2006**, *67*, 1.
(40) Mariño, F.; Baronetti, G.; Laborde, M.; Bion, N.; Le Valant, A.; Epron, F. *Int. J. Hydrogen Energy* **2008**, *33*, 1345.
(41) Lee, H. C.; Kim, D. H. *Catal. Today* **2008**, *132*, 109.
(42) Chung, L. C.; Yeh, C. T. *Catal. Commun* **2008**, *9*, 670.
(43) Moreno, M.; Baronetti, G. T.; Laborde, M. A.; Mariño, F. J. *Int. J. Hydrogen Energy* **2008**, *33*, 3538.
(44) Rodriguez, J. A.; Jirsak, T.; Freitag, A.; Hanson, J. C.; Larese, J. Z.; Chaturvedi, S. *Catal. Lett.* **1999**, *62*, 113.
(45) Bond, G.; Lois, C.; Thompson, D. *Catalysis by Gold*; World Scientific: River Edge, NJ, 2006.
(46) Haruta, M. *Chem. Rec.* **2003**, *3*, 75.
(47) Kung, M. R.; Davis, J.; Kung, H. H. *J. Phys. Chem. C* **2007**, *111*, 11767.
(48) Meyer, R.; Lemire, C.; Shaikhutdinov, S.; Freund, H.-J. *Gold Bull.* **2004**, *37*.
(49) Saltsburg, Fu Q.; Flytzani-Stephanopoulos, M. *Science* **2003**, *301*, 935.
(50) Carrettin, S.; Concepcion, P.; Corma, A.; Nieto, J. M. L.; Puntes, V. F. *Angew. Chem. Intl. Ed.* **2004**, *43*, 2538.
(51) Chen, M.; Goodman, D. W. *Acc. Chem. Res.* **2006**, *39*, 739.
(52) Rainer, D. R.; Goodman, D. W. *J. Mol. Catal. A* **1998**, *131*, 259.
(53) Henry, C. *Surf. Sci. Rep.* **1998**, *31*, 231.
(54) Bäumer, M.; Freund, H.-J. *Prog. Surf. Sci.* **1999**, *61*, 127.
(55) Shaikhutdinov, S.; Meyer, R.; Naschitzki, M.; Bäumer, M.; Freund, H.-J. *Catal. Lett.* **2003**, *86*, 211.
(56) Starr, D. E.; Shaikhutdinov, S. K.; Freund, H.-J. *Top. Catal.* **2005**, *36*, 33.
(57) Lu, J.-L.; Gao, H.-J.; Shaikhutdinov, S.; Freund, H.-J. *Surf. Sci.* **2006**, *600*, 5004.
(58) Lu, J.-L.; Gao, H.-J.; Shaikhutdinov, S.; Freund, H.-J. *Catal. Lett.* **2007**, *114*, 8.
(59) Weststrate, C. J.; Resta, A.; Westerström, R.; Lundgren, E.; Mikkelsen, A.; Andersen, J. N. *J. Phys. Chem. C* **2008**, *112*, 6900.
(60) Lemire, C.; Meyer, R.; Shaikhutdinov, S.; Freund, H.-J. *Surf. Sci.* **2004**, *552*, 27.
(61) Baron, M.; Bondarchuk, O.; Stacchiola, D.; Shaikhutdinov, S.; Freund, H.-J. *J. Phys. Chem. C* **2009**, *113*, 6042.
(62) Castellani, N. J.; Branda, M. M.; Neyman, K. M.; Illas, F. *J. Phys. Chem. C* **2009**, *113*, 4948.
(63) Kundakovic, L.; Flytzani-Stephanopoulos, M. *J. Catal.* **1998**, *179*, 203.
(64) Imamura, S.; Yamada, H.; Utani, K. *Appl. Catal., A* **2000**, *192*, 221.
(65) Bera, P.; Patil, K. C.; Hegde, M. S. *Phys. Chem. Chem. Phys.* **2000**, *2*, 3715.
(66) Pacchioni, G.; Illas, F. In *Catalysis and Electrocatalysis at Nanoparticle Surfaces*; Wieckowski, A., Savinova, E., Vayenas, C. G., Eds.; Marcel Dekker: New York, 2003; pp 65−108.
(67) López, N.; Illas, F. In *Supported Metals in Catalysis*; Fernandez-García, M., Anderson, J. A., Eds.; Imperial College Press, London, 2005; pp 33−73.
(68) Loschen, C.; Carrasco, J.; Neyman, K. M.; Illas, F. *Phys. Rev. B* **2007**, *75*, 035115.
(69) Cococcioni, M.; de Gironcoli, S. *Phys. Rev. B* **2005**, *71*, 035105.
(70) Da Silva, J. L. F.; Ganduglia-Pirovano, M. V.; Sauer, J.; Bayer, V.; Kresse, G. *Phys. Rev. B* **2007**, *75*, 045121.
(71) Hay, P. J.; Martin, R. L.; Uddin, J.; Scuseria, G. E. *J. Chem. Phys.* **2006**, *125*, 034712.
(72) Zhang, C.; Michaelides, A.; King, D. A.; Jenkins, S. J. *J. Chem. Phys.* **2008**, *129*, 194708.
(73) Cruz Hernández, N.; Grau-Crespo, R.; de Leeuw, N. H.; Sanz, J. F. *Phys. Chem. Chem. Phys.* **2009**, *11*, 5246.
(74) Branda, M. M.; Castellani, N. J.; Grau-Crespo, R.; de Leeuw, N. H.; Cruz Hernandez, N.; Sanz, J. F.; Neyman, K. M.; Illas, F. *J. Chem. Phys.* **2009**, *131*, 94702.
(75) Kresse, G.; Hafner, J. *Phys. Rev. B* **1993**, *47*, 558.
(76) Kresse, G.; Hafner, J. *Phys. Rev. B* **1993**, *48*, 13115.
(77) Kresse, G.; Hafner, J. *Phys. Rev. B* **1994**, *49*, 14251.
(78) Blochl, P. *Phys. Rev. B* **1994**, *50*, 17953.
(79) Kresse, G.; Joubert, D. *Phys. Rev. B* **1999**, *59*, 1758.
(80) Anisimov, V. I.; Aryasetiawan, F.; Lichtenstein, A. I. *J. Phys.: Condens. Matter* **1997**, *9*, 767.
(81) Anisimov, V. I.; Solovyev, I. V.; Korotin, M. A.; Czyzyk, M. T.; Sawatzky, G. A. *Phys. Rev. B* **1993**, *48*, 16929.
(82) Solovyev, I. V.; Dederichs, P. H.; Anisimov, V. I. *Phys. Rev. B* **1994**, *50*, 16861.
(83) Vosko, S. H.; Wilk, L.; Nusair, M. *Can. J. Phys.* **1980**, *58*, 1200.
(84) Perdew, J. P.; Chevary, J. A.; Vosko, S. H.; Jackson, K. A.; Pederson, M. R.; Singh, D. J.; Fiolhais, C. *Phys. Rev. B* **1992**, *46*, 6671.
(85) Perdew, J. P.; Chevary, J. A.; Vosko, S. H.; Jackson, K. A.; Pederson, M. R.; Singh, D. J.; Fiolhais, C. *Phys. Rev. B* **1993**, *48*, 4978.
(86) Dudarev, S. L.; Botton, G. A.; Savrasov, S. Y.; Humphreys, C. J.; Sutton, A. P. *Phys. Rev. B* **1998**, *57*, 1505.
(87) Monkhorst, H. J.; Pack, J. D. *Phys. Rev. B* **1976**, *13*, 5188.
(88) Methfessel, M.; Paxton, A. T. *Phys. Rev. B* **1989**, *40*, 3616.
(89) Bader, R. F. W. *Atoms in Molecules*; Oxford University Press: Oxford, 1990.
(90) Loschen, C.; Bromley, S. T.; Neyman, K. M.; Illas, F. *J. Phys. Chem. C* **2007**, *111*, 10142.
(91) Loschen, C.; Migani, A.; Bromley, S. T.; Illas, F.; Neyman, K. M. *Phys. Chem. Chem. Phys.* **2008**, *10*, 5730.
(92) Migani, A.; Loschen, C.; Illas, F.; Neyman, K. M. *Chem. Phys. Lett.* **2008**, *465*, 106.
(93) Migani, A.; Neyman, K M.; Illas, F.; Bromley, S. T. *J. Chem. Phys.* **2009**, *131*, 064701.
(94) Nolan, M.; Grigoleit, S.; Sayle, D. C.; Parker, S. C.; Watson, G. W. *Surf. Sci.* **2005**, *576*, 217.
(95) Duclos, S. J.; Vohra, Y. K.; Ruoff, A. L.; Jayaraman, A.; Espinosa, G. P. *Phys. Rev. B* **1998**, *38*, 7755.
(96) Gerward, L.; Olsen, J. S. *Powder Diffr.* **1993**, *8*, 127.
(97) Giordano, L.; Pacchioni, G.; Bredow, T.; Sanz, J. F. *Surf. Sci.* **2001**, *471*, 21.

(98) Hernández, N. C.; Sanz, J. F. *Phys. Rev. Lett.* **2005**, *94*, 016104.
(99) Hernández, N. C.; Graciani, J.; Márquez, A.; Sanz, J. F. *Surf. Sci.* **2005**, *575*, 189.
(100) Hernández, N. C.; Sanz, J. F. *J. Phys. Chem. B* **2002**, *106*, 11495.
(101) Silvi, B.; Savin, A. *Nature* **1994**, *371*, 683.
(102) Ganduglia-Pirovano, M. V.; Juarez da Silva, L. F.; Sauer, J. *Phys. Rev. Lett.* **2009**, *102*, 026101.
(103) Rodriguez, J. A.; Evans, J.; Graciani, J.; Park, J.-B.; Liu, P.; Hrbek, J.; Sanz, J. F. *J. Phys. Chem. C* **2009**, *113*, 7364.
(104) Zhang, C.; Michaelides, A.; King, D. A.; Jenkins, S. J. *J. Chem. Phys.* **2008**, *129*, 194708.
(105) Morse, M. D. *Chem. Rev.* **1986**, *86*, 1049.
(106) Grönbeck, H.; Broqvist, P. *J. Phys. Chem. B* **2003**, *107*, 12239.
(107) Cruz Hernández, N.; Graciani, J.; Márquez, A.; Sanz, J. F. *Surf. Sci.* **2005**, *575*, 189.
(108) Ferullo, R. M.; Garda, G. R.; Belelli, P. G.; Branda, M. M.; Castellani, N. J. *THEOCHEM* **2006**, *769*, 217.

JP910782R